

Published in final edited form as:

Hypertension. 2012 May ; 59(5): 1060–1068. doi:10.1161/HYPERTENSIONAHA.111.190140.

Poly(ADP-ribose) Polymerase-1 (PARP-1) Inhibition Improves Coronary Arteriole Function in Type 2 Diabetes

Soo-Kyoung Choi¹, Maria Galán¹, Modar Kassan¹, Megan Partyka¹, Mohamed Trebak², and Khalid Matrougui¹

¹Department of Physiology, Hypertension and Renal Center of Excellence, Tulane University, 1430 Tulane Ave., New Orleans, LA, 70112

²Center for Cardiovascular Sciences, Albany Medical College, Albany 12208, New York

Abstract

Type 2 diabetes (T2D) is associated with microvascular dysfunction. We hypothesized that increased Poly - (ADP-ribose) polymerase-1 (PARP-1) activity contributes to microvascular dysfunction in T2D. T2D (db⁻/db⁻) and non-diabetic control (db⁻/db⁺) mice were treated with two different PARP-1 inhibitors (INO-1001, 5 mg/Kg/day and ABT-888, 15 mg/Kg/day) for two weeks. Isolated coronary arterioles (CA) were mounted in an arteriograph. Pressure-induced myogenic tone (MT) was significantly potentiated, while endothelium-dependent relaxation (EDR) was significantly attenuated in diabetic mice compared to control. These results were associated with decreased endothelial nitric oxide synthase (eNOS) phosphorylation, cyclic guanosine 3' 5'-monophosphate (cGMP) level and increased PARP-1 activity in CA from diabetic mice compared to control. Interestingly, PARP-1 inhibitors significantly reduced the potentiation of MT, improved EDR, restored eNOS phosphorylation, cGMP and attenuated cleaved PARP-1. These results were supported by in vitro studies indicating that down-regulation of PARP-1 in mesenteric resistance arteries (MRA) using PARP-1 shRNA lenti-viral particles significantly improved EDR in MRA from diabetic mice compared to control. The inhibition of nitric oxide synthesis by *N*G-nitro-L-arginine methyl ester (L-NAME) significantly reduced the EDR in CA and MRA from control and diabetic mice treated with PARP-1 inhibitors and PARP-1 shRNA lenti-viral particles. In addition, we demonstrated that enhanced cleaved PARP-1, its binding to DNA and DNA damage were reduced after PARP-1 inhibition in cultured endothelial cells stimulated with high glucose. We provide evidence that T2D impairs microvascular function by an enhanced PARP-1 activity-dependent mechanism. Therefore, PARP-1 could be a potential target for overcoming diabetic microvascular complications.

Keywords

poly - (ADP-ribose) polymerase-1 (PARP-1); endothelial dysfunction; coronary arteriole; myogenic tone; endothelium-dependent relaxation

Corresponding Authors: Khalid Matrougui, Ph.D. (kmatroug@tulane.edu), Department of Physiology, Hypertension and Renal Center of Excellence, Tulane University, 1430 Tulane Ave, New Orleans, LA, 70112 Phone: (504)-889-2588, Fax: (504)-988-267.

Conflict(s) of Interest/Disclosure(s)

None

Publisher's Disclaimer: This is a PDF file of an unedited manuscript that has been accepted for publication. As a service to our customers we are providing this early version of the manuscript. The manuscript will undergo copyediting, typesetting, and review of the resulting proof before it is published in its final citable form. Please note that during the production process errors may be discovered which could affect the content, and all legal disclaimers that apply to the journal pertain.

Introduction

Endothelium-dependent relaxation is a major function of the microcirculation. Physiological and pathological regulation of endothelium-dependent relaxation mechanism is fundamental and not yet determined. Clinically, most of morbidity and mortality of diabetes are mostly related to macrovascular and microvascular complications.^{1, 2} Diabetes is a powerful risk factor for coronary artery disease, stroke and peripheral arterial disease.³ It has been reported that endothelial function and myogenic tone are impaired in type 2 diabetes.^{2, 4} Limited studies to reveal the mechanisms underlying vascular dysfunction in diabetes have been conducted.

Poly (ADP-ribose) polymerase -1 (PARP-1) is an abundant nuclear enzyme involved in multiple DNA repair such as single strand breaks, double strand breaks and base excision.^{5, 6} Upon binding to damaged DNA, PARP-1 cleaves nicotine amide adenine dinucleotide (NAD⁺) into nicotinamide and adenosine diphosphate (ADP)-ribose.⁷ When DNA damage is mild, PARP-1 participates in DNA repair process. However, when DNA damage is extensive, PARP-1 is over-activated, which induces depletion of NAD⁺ and ATP levels and leads to cell dysfunction and death.^{8, 9} PARP-1 activation can be triggered by oxidative stress and nitrosative stress, which affects multiple metabolic pathways, transcriptional regulation, and gene expression.¹⁰

Although the involvement of PARP-1 is well documented in the field of cancer research^{11, 12} and it has been reported that endothelial function was improved after PARP-1 inhibition in streptozotocin induced type 1 diabetic mice¹³, the role of PARP-1 and the down stream signaling in vascular function of type 2 diabetic mice is an important question and remains unanswered. Thus, the purpose of this study was to determine the potential therapeutic effect of PARP-1 inhibition to treat impaired vascular function in type 2 diabetic mice. To test our hypothesis, we treated mice with two novel potent PARP-1 inhibitors, INO-1001 and ABT-888.

Methods

Animal models

8 to 10 weeks old type 2 diabetic mice (db⁻/db⁻), which have a mutation in leptin receptor¹⁴ and age matched heterozygote control mice (db⁻/db⁺) were obtained from Jackson Laboratories. Mice were divided into six groups: 1) control mice with no treatment; 2) control mice who received PARP-1 inhibitor (INO-1001, 5 mg/kg/day from mini-osmotic pumps); 3) control mice who received another PARP-1 inhibitor (ABT-888, 15 mg/kg/day from mini-osmotic pumps); 4) diabetic mice without treatment; 5) diabetic mice treated with INO-1001 (5 mg/kg/day from mini-osmotic pumps); 6) diabetic mice treated with ABT-888 (15 mg/kg/day from mini-osmotic pumps). The selection of the dose of PARP-1 inhibitors was based on previous studies.^{15, 16} The chemical name of INO-1001 is 3-aminobenzamide and it is an isoindolinone derivative and potent inhibitor of PARP-1 with chemosensitization and radiosensitization properties.¹⁷ ABT-888, veliparib is (R)-2-(2-methylpyrrolidin-2-yl)-1H-benzo[d]imidazole-4-carboxamide and is also a potent PARP-1 inhibitor.^{18, 19} These studies are conformed to the principles of the National Institutes of Health "Guide for the Care and Use of Laboratory Animals" and approved by Tulane University Institutional Animal Care.

Blood glucose

Blood glucose measurements were obtained from tail blood samples using a blood glucose meter (Prestige Smart System HDI; Home Diagnostic) in all groups of mice after 6 hours fast as previously described.²

Blood pressure

Arterial systolic blood pressure was measured in conscious mice using the CODA tail-cuff blood pressure system (Kent Scientific, Torrington, CT) as previously described.²⁰

Insulin resistance

Insulin resistance was determined by enzyme immunoassay using the Ultrasensitive Mouse Insulin ELISA protocol (Merckodia, Uppsala, Sweden), which estimates steady-state insulin resistance as previously described.²

Preparation of isolated coronary arterioles

After 2 weeks of treatment, mice were sacrificed and coronary arterioles were isolated, cannulated with glass micropipettes and perfused with physiological salt solution (PSS) bubbled with a 95% O₂ + 5% CO₂ gas mixture. The vessels were pressurized to 50 mmHg using pressure-servo control perfusion systems (Living Systems Instruments, St. Albans, Vermont) for 40 min equilibration period. A video image analyzer as previously described monitored the vessel diameter.² Intraluminal pressure was increased from 25 mmHg to 100 mmHg in a stepwise manner to measure myogenic tone. At the end of the experiments, vessels were incubated with a calcium-free PSS to determine passive diameter. Myogenic tone is calculated as the percentage between active and passive diameter. To determine the endothelium-dependent relaxation, pressurized arteries were pre-constricted with thromboxane agonist (U-46619, 10⁻⁷ mol/L) and then, cumulative concentrations (10⁻⁹ mol/L - 10⁻⁵ mol/L) of acetylcholine were applied. Endothelium-dependent relaxation was also performed in the presence of nitric oxide synthase (NOS) inhibitor *N* G-nitro-L-arginine methyl ester (L-NAME; 10⁻⁴ mol/L) added to the superfusate for 30 min before the assessment of the vasodilator response to acetylcholine.

Western blot analysis

Freshly isolated hearts and mesenteric resistance arteries from all groups were immediately frozen in liquid nitrogen and then homogenized in ice-cold lysis buffer as described previously.^{20, 21} Western blot analysis was performed for total endothelial nitric oxide synthase (eNOS, 1:1,000 dilution; Cell Signaling, Boston, MA), phosphorylated eNOS at Ser635 (1:1,000 dilution; Upstate, Billerica, MA) and total and cleaved PARP-1 using specific antibodies (1:1,000 dilution; Cell Signaling, Boston, MA). Blots were stripped and then reprobated with the GAPDH antibody (1:2,000 dilution; Santa Cruz, Santa Cruz, CA) to verify the equal loading between the samples.

Colorimetric determination of cGMP

cGMP levels were measured in heart tissues in all groups of mice. Mice were sacrificed and heart tissues were immediately harvested and frozen in liquid nitrogen. Measurements were performed using a sandwich enzyme-linked immunosorbent assay (cGMP ELISA kit; Cayman Chemical, Ann Arbor, MI) according to the manufacturer instructions and as previously described.²²

Down-regulation of PARP-1 expression in mesenteric resistance artery

Mesenteric resistance arteries were isolated and cleaned of fat and connective tissues. After incubation of arteries with PARP-1 shRNA lenti-viral particle (Santa Cruz, Santa Cruz, CA) for 4 hours, mesenteric resistance arteries were mounted in a myograph to determine endothelium-dependent relaxation as previously described.²⁰

Endothelial cell culture and preparation of nuclear extracts

Mouse coronary arterioles endothelial cells (ECs) were purchased from CelProgen (San Pedro, CA) and cultured according to the manufacturer instructions using complete growth media. Cultured ECs were starved for 24 hours in medium containing normal glucose (NG) and 1 % of fetal bovine serum and then stimulated with 25 mmol/L D-glucose high glucose (HG) for 1 hour. PARP-1 inhibitors (INO-1001, 5 μ mol/L and ABT-888, 5 μ mol/L) were added 1 hour prior to the incubation with HG. Nuclear extracts were prepared as previously described.²³

Immunocytochemistry

Endothelial cells were starved for 24 hours in NG medium containing 1 % of fetal bovine serum (FBS) and then exposed to PARP-1 inhibitors (INO-1001, 5 μ mol/L and ABT-888, 5 μ mol/L) 1 hour prior to the addition of HG for 1 hour. Cells were then washed in PBS, fixed in 4 % paraformaldehyde and incubated with anti cleaved PARP-1 and total PARP-1 antibodies, followed by labeling with secondary antibody anti-mouse and anti-rabbit IgG conjugated to Alexa 594 and to Alexa 488 (Molecular Probes, Carlsbad, CA). After washing, the slides were mounted with SlowFade Gold antifade reagent with DAPI (Molecular Probes, Carlsbad, CA) and immunofluorescent signal was visualized using a fluorescence microscope Eclipse 55i (X20), Nikon. The fluorescent signal was analyzed using the software NIS-Elements BR 3.0 (Nikon, Tokyo, Japan).

Electrophoretic Mobility Shift Assay (EMSA)

Electrophoretic-mobility-shift assays for PARP-1 were performed using nuclear extracts from cultured mouse coronary arterioles ECs. Nuclear cell extracts were incubated with double-strand unlabeled oligonucleotides (*P30F*: 5'-TCGAAGTTGTTCTATCTCGCGAGAGGTTGCCCC-3', and iNOS: 5'-GTAAGAAATTATAATTTATTCGTT-3'), based on the oligonucleotide iNOS described by Yu Z *et al.*,²⁴ containing affinity PARP-1 binding sites. Briefly, both oligonucleotides were annealed to their antisense counterparts and added to 10 μ g of endothelial cells nuclear extracts and the assay was performed using a fluorescence-based Electrophoretic Mobility Shift Assay (EMSA) Kit (Molecular Probes, Carlsbad, CA). After 20 min of incubation at room temperature, the mixture was run on a 6 % polyacrylamide non-denaturing gel (Novex® TBE and DNA Retardation Gels; Invitrogen, Carlsbad, CA) in 0.5 \times TBE (4.45 mmol/L Tris base, 4.45 mmol/L boric acid, 0.2 mmol/L EDTA) for 90 min at room temperature. For supershift, nuclear extracts were pre-incubated for 5 min with anti-PARP-1 (Santa Cruz Biotechnology, Santa Cruz, CA) and 10 μ g of nuclear extracts from cells overexpressing PARP-1 were used as a binding positive control.

DNA damage analysis by Comet assay

The presence of DNA damage was examined by single-cell electrophoresis (Comet assay) using manufacturer's protocol (OxiSelect Comet Assay Kit; Cell Biolabs, Inc. San Diego, CA). Briefly, ECs were stimulated with NG or HG for 24 hours with or without PARP-1 inhibitors. Cells were then harvested and washed with PBS. Cell suspension was mixed with agarose at 37 °C, and then 75 μ L of this mixture was instantly added to comet slides. Slides were immersed in lysis buffer at 4 °C for 1 hour and then replaced with pre-chilled alkaline buffer and placed at 4 °C for 30 minutes followed by electrophoresis (35 V for 15 minutes) in a horizontal electrophoresis chamber filled with Tris borate EDTA (TBE) buffer. Slides were transferred to a container filled with cold water for 2 to 4 minutes and then placed in 70 % ethanol for 5 minutes and air dried overnight at room temperature. After staining with Vista Green DNA dye for 15 minutes at room temperature, comets were observed by

fluorescent microscopy (Nikon, Tokyo, Japan) with X20 magnification. The images were analyzed using the software NIS-Elements BR 3.0 (Nikon, Tokyo, Japan).

Statistical analysis

Results are expressed as mean \pm SEM. One-way or 2-way ANOVA was used to compare each parameter when appropriate. Comparisons between groups were performed with *t*-tests when the ANOVA test was statistically significant. Values of $P < 0.05$ were considered significant. Differences between specified groups were analyzed using the Student's *t* test (two-tailed) for comparing two groups with $P < 0.05$ considered statistically significant.

Results

Effect of PARP-1 inhibition on blood glucose, insulin levels, body weight, and systolic blood pressure

Body weight, blood glucose and insulin levels were increased in diabetic mice compared to control mice and were not affected by INO-1001 or ABT-888 treatments (Figure 1A, B, C). Blood pressure was similar in all groups of mice, which indicates that type 2 diabetic (db⁻/db⁻) mice are normotensive (Figure 1D).

Effect of PARP-1 inhibition on myogenic tone and endothelium-dependent relaxation in coronary arterioles

Myogenic tone was significantly increased in coronary arterioles from type 2 diabetic mice compared to control mice (Figure 2A) and was significantly reduced after PARP-1 inhibition (Figure 2A). The passive diameters at 50 mmHg in all groups of mice were not statistically different ($115.5 \pm 3.4 \mu\text{m}$ for non-treated control mice; $120.2 \pm 10.1 \mu\text{m}$ for control mice treated with INO-1001; $117.2 \pm 10.1 \mu\text{m}$ for control mice treated with ABT-888; $114.2 \pm 12.1 \mu\text{m}$ for non-treated diabetic mice; $118 \pm 9.0 \mu\text{m}$ for diabetic mice treated with INO-1001; and $114.2 \pm 7.9 \mu\text{m}$ for diabetic mice treated with ABT-888). Thromboxane analogue, U46619, induced similar contractions in coronary arterioles from all the groups (data not shown). Endothelium-dependent relaxation was significantly reduced in coronary arterioles from diabetic mice compared to control. Interestingly, endothelium-dependent relaxation was significantly improved in coronary arterioles from diabetic mice treated with PARP-1 inhibitors. The endothelium-dependent relaxation of coronary arterioles was shifted to the left in control mice treated with ABT-888 (Figure 2B). The $-\log \text{EC}_{50}$ s of ACh in all groups of mice were not statistically different (5.96 ± 0.18 for non-treated control mice; 6.43 ± 0.13 for control mice treated with INO-1001; 7.44 ± 0.11 for control mice treated with ABT-888; 6.9 ± 0.08 for non-treated diabetic mice; 6.45 ± 0.2 for diabetic mice treated with INO-1001; and 6.18 ± 0.31 for diabetic mice treated with ABT-888). The endothelium-dependent relaxation in coronary arterioles in the presence of nitric oxide synthase inhibitor (N_{ω} -Nitro-L-arginine methyl ester, L-NAME) was similar in all groups of mice (Figure 2C). The $-\log \text{EC}_{50}$ s for ACh in the presence of L-NAME were similar in all groups of mice (7.00 ± 0.49 for non-treated control mice; 7.66 ± 0.29 for control mice treated with INO-1001; 7.00 ± 0.34 for control mice treated with ABT-888; 7.50 ± 0.13 for non-treated diabetic mice; 6.06 ± 0.16 for diabetic mice treated with INO-1001; and 7.04 ± 0.27 for diabetic mice treated with ABT-888). The endothelium-dependent relaxation in the presence of L-NAME was associated with reduced eNOS phosphorylation at Ser 635 and expression in coronary arterioles in diabetic mice (Figure 2D). Importantly, eNOS phosphorylation and expression were restored in coronary arterioles after treatment with PARP-1 inhibitors (Figure 2D). In Figure 2D, phosphorylated eNOS at Ser635 and total eNOS were standardized to GAPDH. The results were also presented as follow: total eNOS was standardized to GAPDH and then phosphorylated eNOS was standardized to total eNOS/GAPDH (phosphorylated eNOS/total eNOS/GAPDH). The

results of eNOS western blot data were supported by cGMP measurements, indicating that PARP-1 inhibition restores cGMP level to the normal level (Figure 2E).

Effect of PARP-1 inhibition on cleaved and total PARP-1 levels on endothelium-dependent relaxation in coronary arteriole

Cleaved PARP-1 level was increased in heart tissues from diabetic mice compared to control mice. The treatment with INO-1001 or ABT-888 did not affect cleaved PARP-1 levels in control group. However, INO-1001 and ABT-888 significantly decreased cleaved PARP-1 levels in diabetic mice (Figure 2F). Total PARP-1 level was also increased in diabetic mice and was not affected by PARP-1 inhibitors (Figure 2F).

Effect of PARP-1 down regulation by PARP-1 shRNA lenti-viral particle on endothelium-dependent relaxation in mesenteric resistance artery

We down-regulated PARP-1 expression in MRA by incubating them with PARP-1 shRNA lenti-viral particles. PARP-1 shRNA lenti-viral particles significantly reduced PARP-1 expression as evidenced by western blot analysis (Figure 3A). Interestingly, down-regulation of PARP-1 expression significantly improved endothelium-dependent relaxation in mesenteric resistance arteries in diabetic mice, while no effect was observed in mesenteric resistance arteries from control mice (Figure 3B, C). The inhibition of nitric oxide (NO) synthesis greatly reduced endothelium-dependent relaxation in mesenteric resistance arteries from diabetic mice and control mice subjected to PARP-1 shRNA lenti-viral particles (Figure 3B, C).

Effect of high glucose on PARP-1 activity, its binding to DNA, and DNA damage

Primary cultured ECs from coronary arterioles with HG stimulation showed an increase in cleaved PARP-1 evidenced by western blot analysis in nuclear fractions, immunostaining and EMSA analysis (Figure 4). The level of cleaved PARP-1 was increased in the nuclear extracts after incubation of ECs with HG, and was reduced in the presence of INO-1001 and ABT-888 (Figure 4A). In the cytoplasmic fraction, cleaved PARP-1 was not detected (data not shown). Total PARP-1 level was also increased in nuclear extracts after incubation with high glucose but was not affected by PARP-1 inhibitors (Figure 4A). We also demonstrated using immunofluorescence signal that cleaved PARP-1 was increased after incubation with HG, and was reduced when cells were pre-treated with PARP-1 inhibitors (Figure 4B). Similarly, total PARP-1 signal was also increased in the presence of HG and was not altered after pre-treatment with PARP-1 inhibitors (Figure 4B). Nuclear extracts of ECs incubated with HG showed higher DNA-binding activity. Pre-treated cells with PARP-1 inhibitors induced a marked decrease in the DNA-binding activity of PARP-1 (Figure 4C). The effect of HG and PARP-1 inhibition on DNA strand breaks was determined using the Comet single cell electrophoresis assay. After stimulation of ECs with HG for 24 hours, there was a significant increase in the length of the DNA tails by 2 folds compared to control cells (Figure 4D). The pre-treatment of ECs with PARP-1 inhibitors significantly reduced the length of tails induced by HG (Figure 4D).

Discussion

Impaired microvascular function is an early event in the development of cardiovascular diseases. In this study, we found that elevated PARP-1 activity is responsible for microvascular dysfunction in type 2 diabetic mice. Importantly, the inhibition of PARP-1 activity reduces myogenic tone and improves endothelium-dependent relaxation in coronary arterioles and mesenteric resistance arteries in type 2 diabetic mice. It has been reported that PARP-1 isoform is implicated in the pathogenesis of diabetes mellitus^{25, 26} and diabetic

complications including peripheral neuropathy.^{27, 28} However, the role and mechanisms of PARP-1 up-regulation in microvascular dysfunction in type 2 diabetes remain unclear.

In this study, we found that myogenic tone was elevated and endothelium-dependent relaxation was attenuated in diabetic mice. This finding was associated with a decrease in eNOS phosphorylation, expression, and cGMP level. Our data are in agreement with previous data showing elevated myogenic tone^{2, 29} and impaired endothelial function in diabetic mice.^{30, 31} Interestingly, PARP-1 inhibition restored eNOS phosphorylation at Ser 635 and expression, and cGMP level, associated with normalized myogenic tone and improved endothelium-dependent relaxation in diabetic mice. These data suggest that exacerbated PARP-1 activation is responsible for microvascular dysfunction. It has been reported that PARP-1 mediated endothelial dysfunction in diabetes is related to hyperglycemia.¹³ High glucose induces a significant PARP-1-dependent changes in ATP content and NADPH.¹³ Previous study suggested that the depletion of NAD⁺ in endothelial cells exposed to high glucose is directly responsible for the inhibition of eNOS activity and the impairment of vascular endothelium-dependent relaxation in diabetes.¹³ Our data are in agreement since eNOS activity was significantly reduced and treatment with PARP-1 inhibitors recovered eNOS activity in type 2 diabetic mice. These data suggest that eNOS expression and phosphorylation at Ser635 are regulated by PARP-1 activity; however, the mechanism is still unclear.

It is known that during extensive cell damage, PARP-1 can be cleaved into two fragments which are p89 and p24.^{32, 33} In the present study, we found an increase in the 24 kDa fragment of cleaved PARP-1 from diabetic mice compared to control mice, which are suppressed by PARP-1 inhibitors while total PARP-1 levels were not affected.

To further demonstrate the role of PARP-1 in microvascular function, we down-regulated PARP-1 expression and found an improvement in endothelium-dependent relaxation in mesenteric resistance arteries from diabetic mice. Thus, our data suggest that although DNA repair is withheld, the overall tissue damage exposed to hyperglycemia may be reduced by PARP-1 inhibition. These findings are in agreement with previous studies reporting that PARP-1 deficient mice are resistant to streptozotocin-induced diabetes.^{34, 35}

To support the functional studies, we performed *in vitro* studies with ECs exposed to HG to simulate *in vivo* condition of diabetes. Nuclear fractions of ECs were subjected to western blot analysis and the results indicated an increase in cleaved PARP-1 in cells exposed to HG. Cleaved PARP-1, detected in nuclear fraction but not in the cytoplasmic fraction, was increased in endothelial cells exposed to HG and was decreased in the presence of INO-1001 and ABT-888. The expression of total PARP-1 was also augmented in nuclear extracts but was not altered with PARP-1 inhibitors. These data correlate with EMSA analysis indicating that HG stimulation showed higher DNA-binding activity. Pre-treated cells with INO-1001 and ABT-888 reduced the DNA-binding activity of PARP-1. According to a previous report, a significant poly - (ADP-ribose) immunostaining was found in microvessels of diabetic retinae.³⁶ In the present study, we demonstrated that cleaved PARP-1 and total PARP-1 were increased in cells stimulated with HG. Inhibition of PARP-1 activity significantly reduced cleaved PARP-1 fluorescence in the nuclei of cells stimulated with HG, but it did not affect the total PARP-1. These data correlate with our *in vivo* study and are also in agreement with previous studies reporting that pretreatment of animals with PARP-1 inhibitors reduced PARP-1 activity and protected against streptozotocin-induced β -cell necrosis and hyperglycemia.^{37, 38}

The comet assay has been extensively used to detect DNA damage induced by various stimuli.³⁹ In our study, pretreatment with PARP-1 inhibitors reduced the length of the comet

tail induced by HG suggesting that the reduction in the exacerbation of PARP-1 activity could protect the cells from an excessive DNA damage.

Our findings indicate that elevated PARP-1 activity is responsible for impaired endothelium-dependent relaxation and potentiation of myogenic tone in type 2 diabetes. Importantly, *in vivo* and *in vitro* inhibition of PARP-1 improved microvascular function in type 2 diabetes. Therefore, PARP-1 inhibition could be a potential strategy to overcome type 2 diabetes-induced vascular dysfunction.

Acknowledgments

N/A

Source(s) of Funding

We acknowledge grant support from National Institutes of Health (1R01HL095566; PI: Dr. Matrougui; 5R01HL097111- PI: Dr. Trebak)

References

1. Brownlee M. Biochemistry and molecular cell biology of diabetic complications. *Nature*. 2001; 414:813–820. [PubMed: 11742414]
2. Belmadani S, Palen DI, Gonzalez-Villalobos RA, Boulares HA, Matrougui K. Elevated epidermal growth factor receptor phosphorylation induces resistance artery dysfunction in diabetic db/db mice. *Diabetes*. 2008; 57:1629–1637. [PubMed: 18319304]
3. Entabi F, Albadawi H, Stone DH, Sroufe R, Conrad MF, Watkins MT. Hind limb ischemia-reperfusion in the leptin receptor deficient (db/db) mouse. *J Surg Res*. 2007; 139:97–105. [PubMed: 17292407]
4. Fitzgerald SM, Kemp-Harper BK, Tare M, Parkington HC. Role of endothelium-derived hyperpolarizing factor in endothelial dysfunction during diabetes. *Clin Exp Pharmacol Physiol*. 2005; 32:482–487. [PubMed: 15854163]
5. Sodhi RK, Singh N, Jaggi AS. Poly(adp-ribose) polymerase-1 (parp-1) and its therapeutic implications. *Vascular pharmacology*. 2010; 53:77–87. [PubMed: 20633699]
6. Burkle A. Physiology and pathophysiology of poly(adp-ribosylation). *Bioessays*. 2001; 23:795–806. [PubMed: 11536292]
7. Nguewa PA, Fuertes MA, Alonso C, Perez JM. Pharmacological modulation of poly(adp-ribose) polymerase-mediated cell death: Exploitation in cancer chemotherapy. *Mol Pharmacol*. 2003; 64:1007–1014. [PubMed: 14573748]
8. Chiarugi A, Moskowitz MA. Cell biology. Parp-1--a perpetrator of apoptotic cell death? *Science*. 2002; 297:200–201. [PubMed: 12114611]
9. Kirkland JB. Poly adp-ribose polymerase-1 and health. *Exp Biol Med (Maywood)*. 2010; 235:561–568. [PubMed: 20463295]
10. Giansanti V, Dona F, Tillhon M, Scovassi AI. Parp inhibitors: New tools to protect from inflammation. *Biochem Pharmacol*. 2010; 80:1869–1877. [PubMed: 20417190]
11. Annunziata CM, O'Shaughnessy J. Poly (adp-ribose) polymerase as a novel therapeutic target in cancer. *Clin Cancer Res*. 2010; 16:4517–4526. [PubMed: 20823142]
12. Chalmers AJ. The potential role and application of parp inhibitors in cancer treatment. *Br Med Bull*. 2009; 89:23–40. [PubMed: 19208614]
13. Garcia Soriano F, Virag L, Jagtap P, Szabo E, Mabley JG, Liaudet L, Marton A, Hoyt DG, Murthy KG, Salzman AL, Southan GJ, Szabo C. Diabetic endothelial dysfunction: The role of poly(adp-ribose) polymerase activation. *Nat Med*. 2001; 7:108–113. [PubMed: 11135624]
14. Van den Bergh A, Flameng W, Herijgers P. Type ii diabetic mice exhibit contractile dysfunction but maintain cardiac output by favourable loading conditions. *Eur J Heart Fail*. 2006; 8:777–783. [PubMed: 16716661]

15. Szabo C, Pacher P, Zsengeller Z, Vaslin A, Komjati K, Benko R, Chen M, Mabley JG, Kollai M. Angiotensin ii-mediated endothelial dysfunction: Role of poly(adp-ribose) polymerase activation. *Mol Med*. 2004; 10:28–35. [PubMed: 15502880]
16. Donawho CK, Luo Y, Penning TD, Bauch JL, Bouska JJ, Bontcheva-Diaz VD, Cox BF, DeWeese TL, Dillehay LE, Ferguson DC, Ghoreishi-Haack NS, Grimm DR, Guan R, Han EK, Holley-Shanks RR, Hristov B, Idler KB, Jarvis K, Johnson EF, Kleinberg LR, Klinghofer V, Lasko LM, Liu X, Marsh KC, McGonigal TP, Meulbroek JA, Olson AM, Palma JP, Rodriguez LE, Shi Y, Stavropoulos JA, Tsurutani AC, Zhu GD, Rosenberg SH, Giranda VL, Frost DJ. Abt-888, an orally active poly(adp-ribose) polymerase inhibitor that potentiates DNA-damaging agents in preclinical tumor models. *Clin Cancer Res*. 2007; 13:2728–2737. [PubMed: 17473206]
17. Hauser B, Groger M, Ehrmann U, Albicini M, Bruckner UB, Schelzig H, Venkatesh B, Li H, Szabo C, Speit G, Radermacher P, Kick J. The parp-1 inhibitor ino-1001 facilitates hemodynamic stabilization without affecting DNA repair in porcine thoracic aortic cross-clamping-induced ischemia/reperfusion. *Shock*. 2006; 25:633–640. [PubMed: 16721272]
18. Jagtap PG, Baloglu E, Southan GJ, Mabley JG, Li H, Zhou J, van Duzer J, Salzman AL, Szabo C. Discovery of potent poly(adp-ribose) polymerase-1 inhibitors from the modification of indeno[1,2-c]isoquinolinone. *J Med Chem*. 2005; 48:5100–5103. [PubMed: 16078828]
19. Albert JM, Cao C, Kim KW, Willey CD, Geng L, Xiao D, Wang H, Sandler A, Johnson DH, Colevas AD, Low J, Rothenberg ML, Lu B. Inhibition of poly(adp-ribose) polymerase enhances cell death and improves tumor growth delay in irradiated lung cancer models. *Clin Cancer Res*. 2007; 13:3033–3042. [PubMed: 17505006]
20. Kassan M, Galan M, Partyka M, Trebak M, Matrougui K. Interleukin-10 released by cd4+cd25+ natural regulatory t cells improves microvascular endothelial function through inhibition of nadph oxidase activity in hypertensive mice. *Arterioscler Thromb Vasc Biol*. 2011; 31:2534–2542. [PubMed: 21817097]
21. Matrougui K, Abd Elmageed Z, Kassan M, Choi S, Nair D, Gonzalez-Villalobos RA, Chentoufi AA, Kadowitz P, Belmadani S, Partyka M. Natural regulatory t cells control coronary arteriolar endothelial dysfunction in hypertensive mice. *Am J Pathol*. 2011; 178:434–441. [PubMed: 21224080]
22. Crawford JH, Chacko BK, Pruitt HM, Piknova B, Hogg N, Patel RP. Transduction of nobioactivity by the red blood cell in sepsis: Novel mechanisms of vasodilation during acute inflammatory disease. *Blood*. 2004; 104:1375–1382. [PubMed: 15150083]
23. Navas MA, Munoz-Elias EJ, Kim J, Shih D, Stoffel M. Functional characterization of the modyl gene mutations hnf4(r127w), hnf4(v255m), and hnf4(e276q). *Diabetes*. 1999; 48:1459–1465. [PubMed: 10389854]
24. Yu Z, Kuncewicz T, Dubinsky WP, Kone BC. Nitric oxide-dependent negative feedback of parp-1 trans-activation of the inducible nitric-oxide synthase gene. *J Biol Chem*. 2006; 281:9101–9109. [PubMed: 16464859]
25. Jagtap P, Szabo C. Poly(adp-ribose) polymerase and the therapeutic effects of its inhibitors. *Nat Rev Drug Discov*. 2005; 4:421–440. [PubMed: 15864271]
26. Virag L. Structure and function of poly(adp-ribose) polymerase-1: Role in oxidative stress-related pathologies. *Curr Vasc Pharmacol*. 2005; 3:209–214. [PubMed: 16026317]
27. Obrosova IG, Li F, Abatan OI, Forsell MA, Komjati K, Pacher P, Szabo C, Stevens MJ. Role of poly(adp-ribose) polymerase activation in diabetic neuropathy. *Diabetes*. 2004; 53:711–720. [PubMed: 14988256]
28. Obrosova IG, Xu W, Lyzogubov VV, Ilnytska O, Mashtalir N, Vareniuk I, Pavlov IA, Zhang J, Slusher B, Drel VR. Parp inhibition or gene deficiency counteracts intraepidermal nerve fiber loss and neuropathic pain in advanced diabetic neuropathy. *Free Radic Biol Med*. 2008; 44:972–981. [PubMed: 17976390]
29. Lagaud GJ, Masih-Khan E, Kai S, van Breemen C, Dube GP. Influence of type ii diabetes on arterial tone and endothelial function in murine mesenteric resistance arteries. *J Vasc Res*. 2001; 38:578–589. [PubMed: 11740157]
30. Avogaro A, Fadini GP, Gallo A, Pagnin E, de Kreutzenberg S. Endothelial dysfunction in type 2 diabetes mellitus. *Nutr Metab Cardiovasc Dis*. 2006; 16(Suppl 1):S39–45. [PubMed: 16530129]

31. Komers R, Schutzer WE, Reed JF, Lindsley JN, Oyama TT, Buck DC, Mader SL, Anderson S. Altered endothelial nitric oxide synthase targeting and conformation and caveolin-1 expression in the diabetic kidney. *Diabetes*. 2006; 55:1651–1659. [PubMed: 16731827]
32. de Murcia G, Menissier de Murcia J. Poly(adp-ribose) polymerase: A molecular nick-sensor. *Trends Biochem Sci*. 1994; 19:172–176. [PubMed: 8016868]
33. Kim MY, Zhang T, Kraus WL. Poly(adp-ribosyl)ation by parp-1: ‘Par-laying’ nad+ into a nuclear signal. *Genes Dev*. 2005; 19:1951–1967. [PubMed: 16140981]
34. Burkart V, Wang ZQ, Radons J, Heller B, Herceg Z, Stingl L, Wagner EF, Kolb H. Mice lacking the poly(adp-ribose) polymerase gene are resistant to pancreatic beta-cell destruction and diabetes development induced by streptozocin. *Nat Med*. 1999; 5:314–319. [PubMed: 10086388]
35. Pieper AA, Brat DJ, Krug DK, Watkins CC, Gupta A, Blackshaw S, Verma A, Wang ZQ, Snyder SH. Poly(adp-ribose) polymerase-deficient mice are protected from streptozotocin-induced diabetes. *Proc Natl Acad Sci U S A*. 1999; 96:3059–3064. [PubMed: 10077636]
36. Butler R, Morris AD, Belch JJ, Hill A, Struthers AD. Allopurinol normalizes endothelial dysfunction in type 2 diabetics with mild hypertension. *Hypertension*. 2000; 35:746–751. [PubMed: 10720589]
37. Mendola J, Wright JR Jr, Lacy PE. Oxygen free-radical scavengers and immune destruction of murine islets in allograft rejection and multiple low-dose streptozocin-induced insulinitis. *Diabetes*. 1989; 38:379–385. [PubMed: 2521836]
38. Masiello P, Novelli M, Fierabracci V, Bergamini E. Protection by 3-aminobenzamide and nicotinamide against streptozotocin-induced beta-cell toxicity in vivo and in vitro. *Res Commun Chem Pathol Pharmacol*. 1990; 69:17–32. [PubMed: 2145620]
39. Vijayalaxmi, Tice RR, Strauss GH. Assessment of radiation-induced DNA damage in human blood lymphocytes using the single-cell gel electrophoresis technique. *Mutat Res*. 1992; 271:243–252. [PubMed: 1378197]

Perspectives

Diabetes is a metabolic disease associated with vascular complication including impaired micro-vascular endothelium-dependent relaxation and myogenic reactivity. Most of clinical studies indicate that patients with type 2 diabetes are high risk for cardiovascular diseases. Although the clinical management of type 2 diabetes has advanced substantially, cardiovascular diseases in patients with type 2 diabetes still constitute a major and increasing health burden worldwide. Despite treatments have progressed, the development of novel effective treatments for patients with vascular complications in type 2 diabetes remain a major research goal. Therefore, there is a significant medical need to develop novel therapies to restore micro-vascular endothelial function, especially in patients with type 2 diabetes. Our results indicate that elevated PARP-1 activity impairs vascular function in type 2 diabetic mice. Interestingly, inhibition of PARP-1 activity improves micro-vascular function through restoration of eNOS, cGMP pathway. Therefore, PARP-1 could be a potential target for a therapeutic strategy to improve vascular function in diabetes.

Novelty and Significance

1) What Is New?

This is the first in vivo study to demonstrate that increased PARP-1 activity is involved in impaired microvascular endothelium-dependent relaxation in type 2 diabetes.

2) What Is Relevant?

This study is relevant because identifying PARP-1 in the complex system that regulates vascular function has the potential to lead to development of new therapeutic strategies to overcome an important vasculopathy in type 2 diabetes.

3) Summary

Type 2 diabetes is associated with enhanced vascular PARP-1 activity and impaired coronary arterioles function. Interestingly, the in vivo inhibition of PARP-1 activity reduced PARP-1 activity and improved coronary arterioles function.

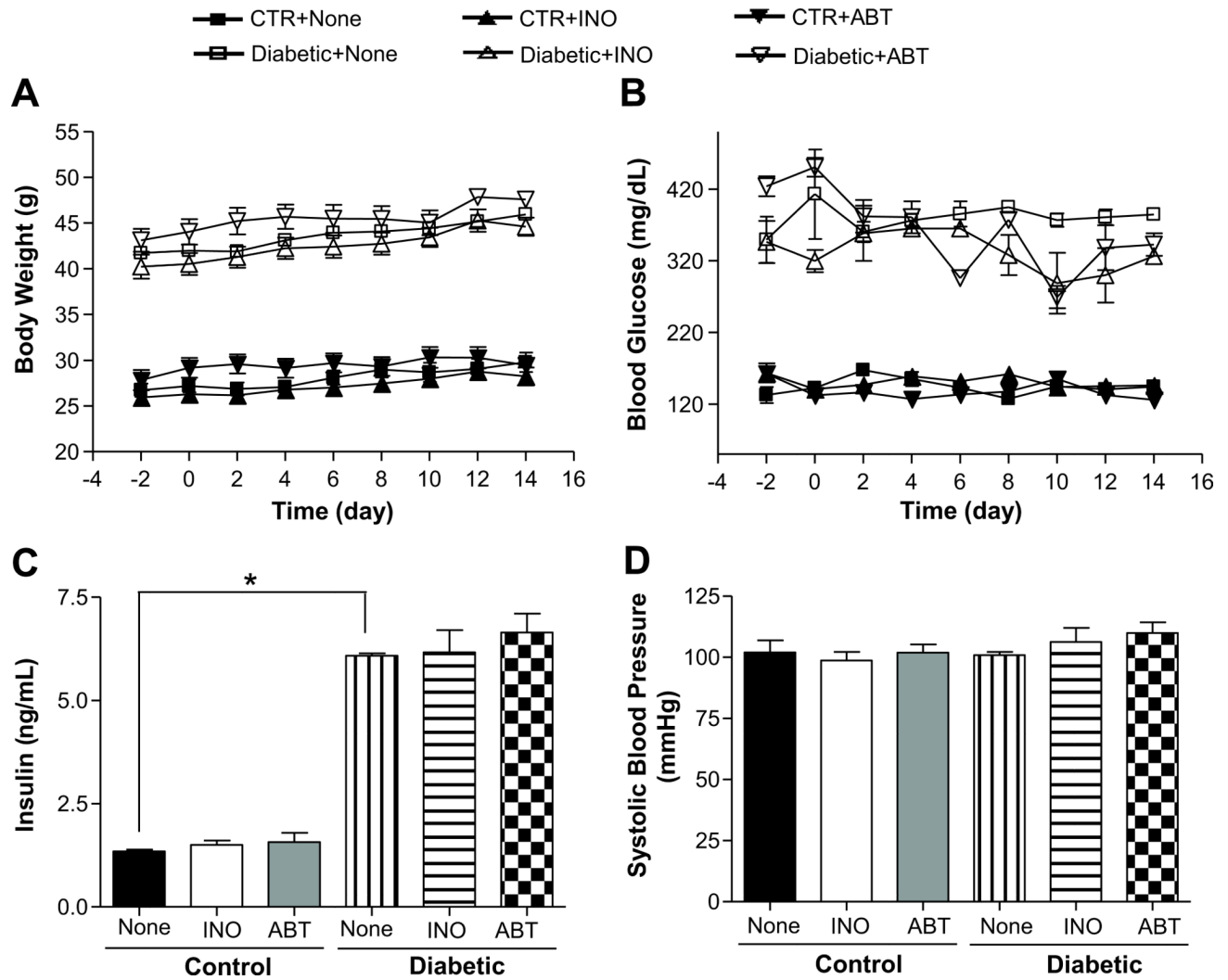


Figure 1. Effect of PARP-1 inhibition on body weight, blood glucose and insulin levels, and blood pressure in control and diabetic mice. **A)** Comparison of blood glucose levels between control and diabetic mice with or without INO-1001 or ABT-888, n=10; **B)** Comparison of body weight between control and diabetic mice with or without INO-1001 or ABT-888, n=10; **C)** Serum insulin levels in all groups, n=10; **D)** Blood pressure measurements with tail-cuff methods in all groups, n=10; *p< 0.05 for diabetic vs. control mice.

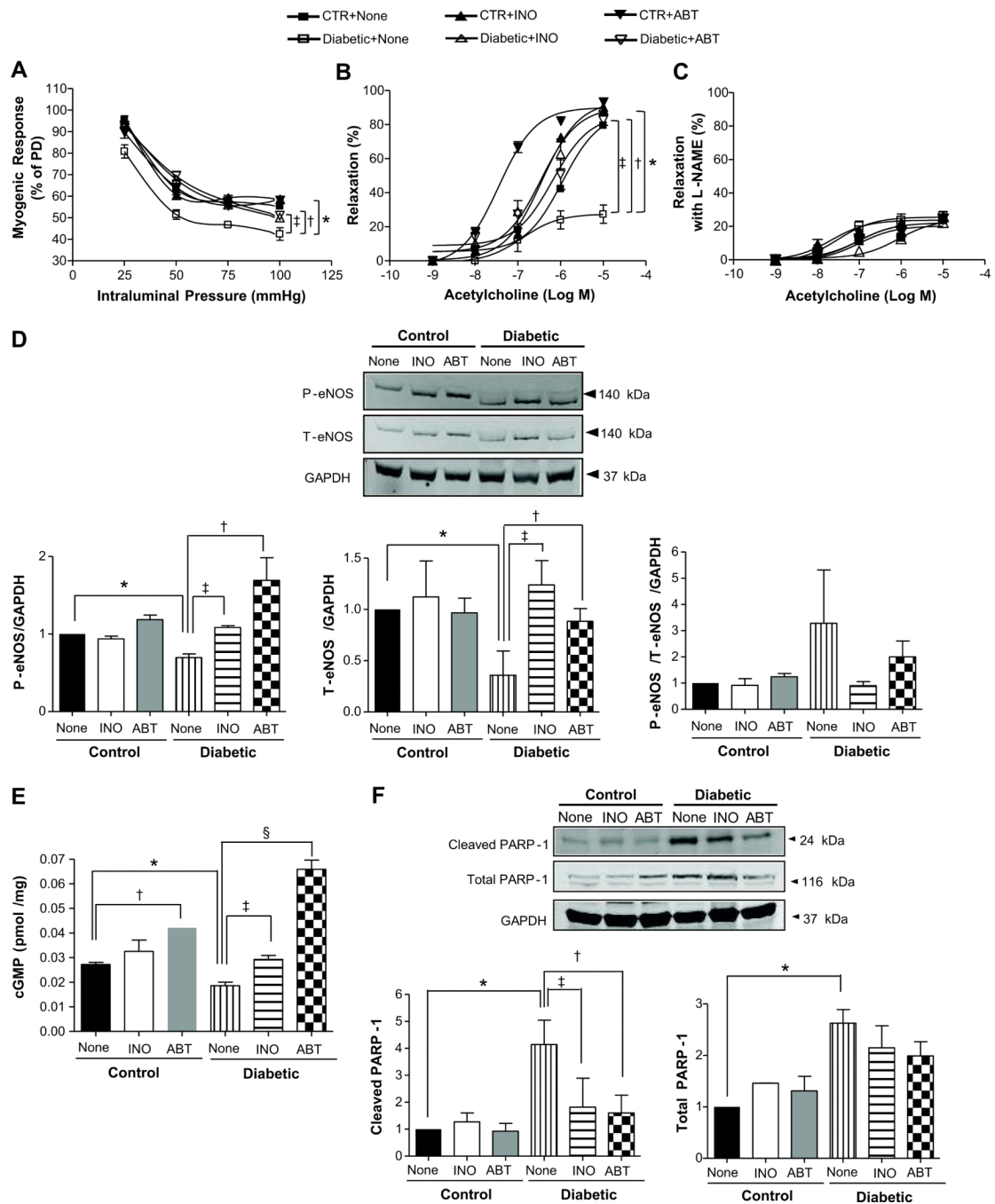


Figure 2.

Effect of PARP-1 inhibitors on myogenic tone and endothelium-dependent relaxation in coronary arterioles. A) Pressure-induced myogenic responses in coronary arteries from all groups treated with or without PARP-1 inhibitors (INO-1001, 5 mg/kg/day or ABT-888, 15 mg/kg/day). * $P < 0.05$ for diabetic vs. control mice; ‡ $P < 0.05$ for diabetic vs. diabetic mice treated with INO-1001; † $P < 0.05$ for diabetic vs. diabetic mice treated with ABT-888, $n=5$; B) Changes in diameter in response to dose-response (10^{-9} to 10^{-5} mol/L) of acetylcholine in coronary artery from all groups of mice. * $P < 0.05$ for diabetic vs. control mice; ‡ $P < 0.05$ for diabetic vs. diabetic mice treated with INO-1001; † $P < 0.05$ for diabetic vs. diabetic mice treated with ABT-888, $n=5$; C) Changes in diameter in response to dose response (10^{-9}

to 10^{-5} mol/L) of acetylcholine with pre-treatment of exogenous nitric oxide synthase inhibitor (*N*_ω-Nitro-L-arginine methyl ester, L-NAME) in coronary arterioles from all groups of mice. $P > 0.05$, n=5; D) Western blot analysis for phosphorylated and total eNOS from all groups. * $P < 0.05$ for diabetic vs. control mice; ‡ $P < 0.05$ for diabetic vs. diabetic mice treated with INO-1001; † $P < 0.05$ for diabetic vs. diabetic mice treated with ABT-888, n=5. E) cGMP levels from all mice group. * $P < 0.05$ for control vs. diabetic mice; † $P < 0.05$ for control mice vs. control mice treated with ABT-888; § $P < 0.05$ for diabetic vs. diabetic mice treated with ABT-888; ‡ $P < 0.05$ for diabetic vs. diabetic mice treated with INO-1001, n=5; F) Detection of cleaved PARP-1 and total PARP-1 proteins from all groups. Bars indicate the quantification of the blots by densitometric analysis relative to GAPDH expression. * $P < 0.05$ for control vs. diabetic mice; ‡ $P < 0.05$ for diabetic vs. diabetic mice treated with INO-1001; † $P < 0.05$ for diabetic vs. diabetic mice treated with ABT-888, n=5.

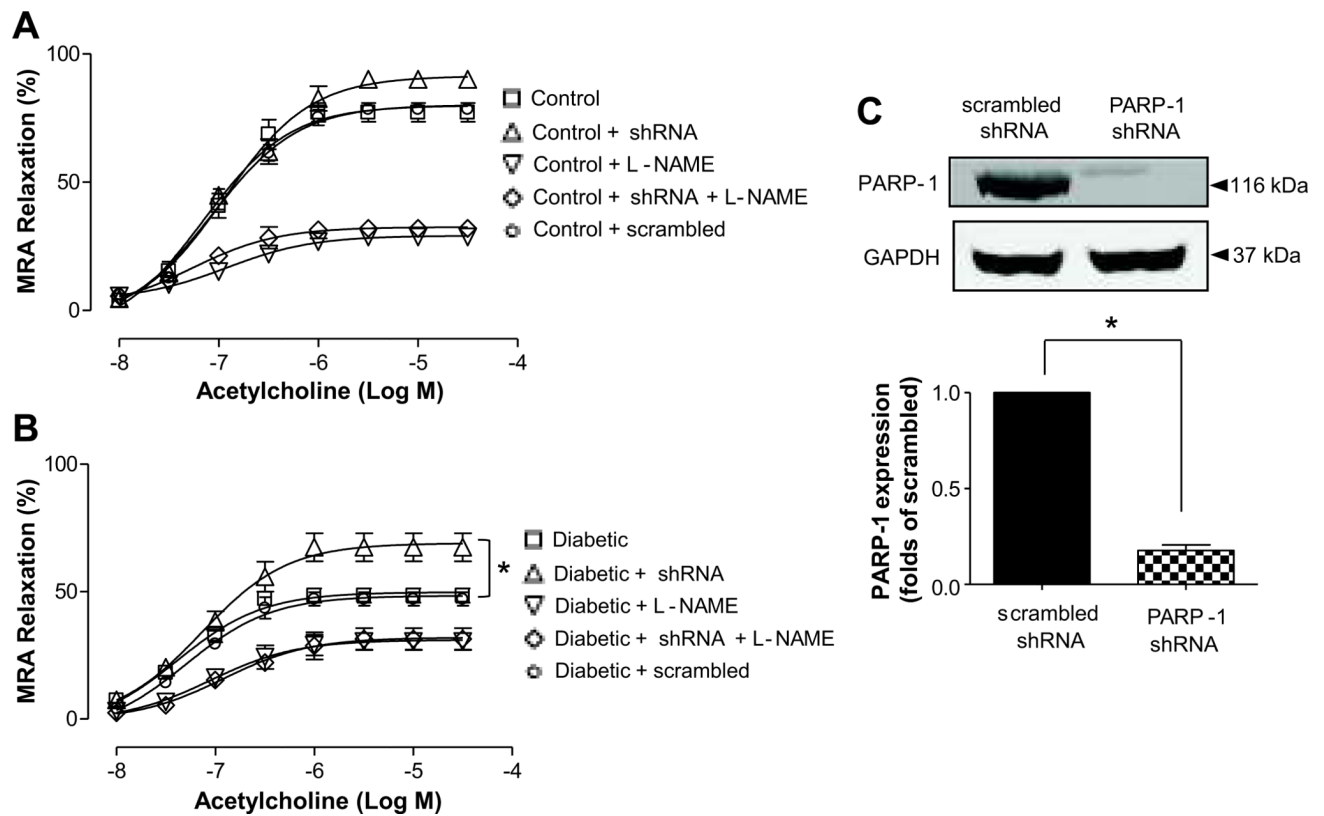


Figure 3.

Effects of PARP-1 shRNA lenti-virus particle on endothelium-dependent relaxation in mesenteric resistance arteries (MRA). A) Changes in diameter in response to dose-response (10^{-8} to 10^{-4} mol/L) of acetylcholine in mesenteric resistance arteries (MRA) from control mice, n=4; B) Changes in diameter in response to dose-response (10^{-8} to 10^{-4} mol/L) of acetylcholine in MRAs from diabetic mice, *P < 0.05, n=5; C) Western blot analysis showing the effects of PARP-1 shRNA lenti-virus particle on the expression of PARP-1 protein, * P < 0.05, n=5.

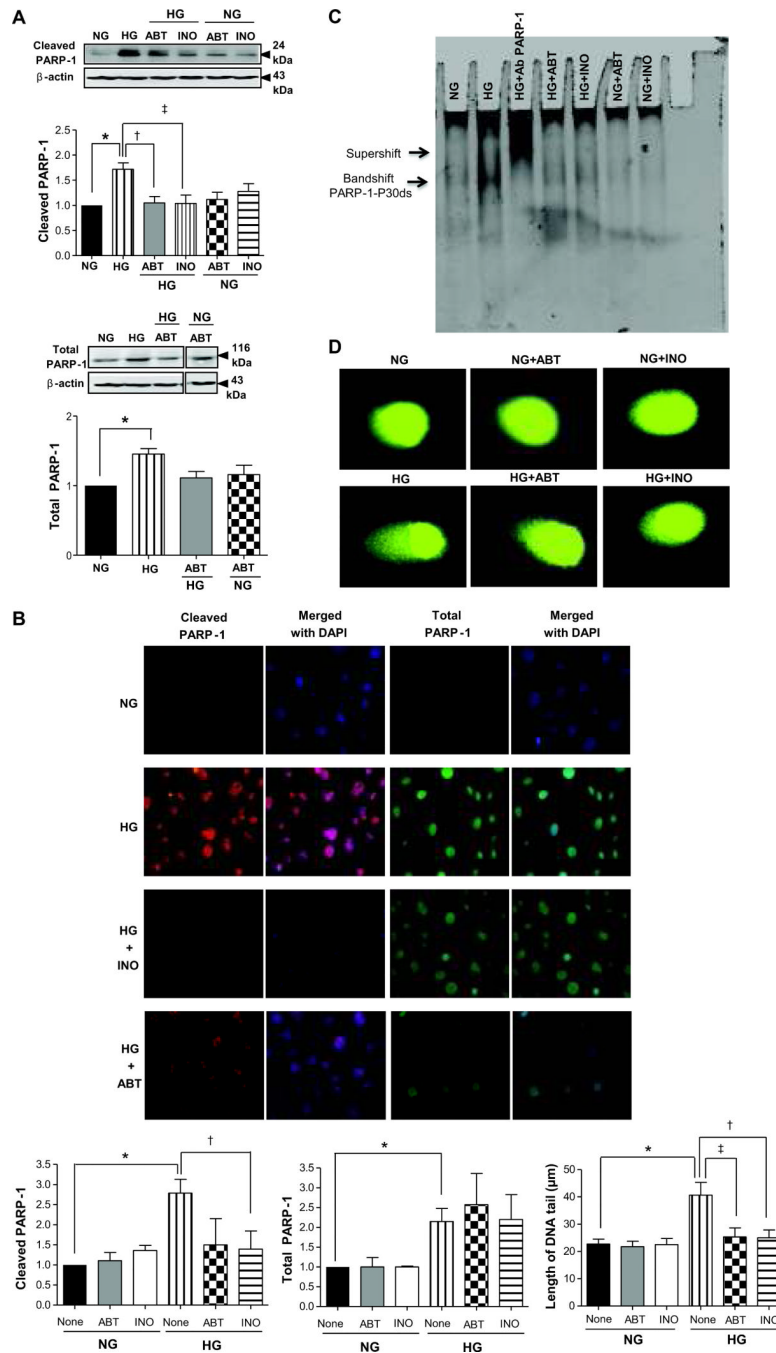


Figure 4. Effects of PARP-1 inhibition in cultured endothelial cells stimulated with high glucose (HG). **A**) Cleaved PARP-1 and total PARP-1 detected in nuclear fraction. Bars indicate the quantification of the blots by densitometric analysis relative to β -actin expression, * $P < 0.05$ for normal glucose (NG) vs. high glucose (HG); † $P < 0.05$ for HG vs. HG with ABT-888; ‡ $P < 0.05$ for HG vs. HG with INO-1001, $n=4$; **B**) Immunofluorescence staining was performed using anti-cleaved PARP-1 rabbit polyclonal antibody (red) and anti-PARP-1 mouse monoclonal antibody (green) in cells untreated or treated with PARP-1 inhibitors 1 h prior to incubation with or without HG for 1 h. Bars indicate the quantification of fluorescence signal inside the nucleus normalized to the signal detected in control cells, * $P <$

0.05 for NG vs. HG; †P < 0.05 for HG vs. HG with INO-1001; n=3; C) Representative EMSA analysis for PARP-1 binding to DNA: the double arrow indicates the PARP-1 bandshift and the upper arrow indicates the supershift; D) Representative comet assay images of endothelial cells incubated with NG of HG treated with or without PARP-1 inhibitors. Measuring 50 cells per experiment for each condition determined mean length of the DNA tails, n=4, *P<0.05 for NG vs. HG; †P<0.05 for HG vs. HG with INO-1001, ‡P<0.05 for HG vs. HG with ABT-888.